Rejecting pressure fluctuations induced by string movement in drilling ⋆

Timm Strecker * **Ole Morten Aamo** *

* *Department of Engineering Cybernetics, NTNU, Norwegian University of Science and Technology, Trondheim N-7491, Norway (e-mail: timm.strecker@itk.ntnu.no; aamo@ntnu.no).*

Abstract: Keeping the pressure within predefined bounds is essential for the safety of managed pressure drilling operations, but drill string movements can induce pressure fluctuations that violate these margins. We extend previous results on disturbance rejection for a 2×2 hyperbolic model of the fluid dynamics in the borehole. We perform a simulation study, in which we illustrate the controller performance for heave induced oscillations and compare it to the previously available controller. The stochasticity of sea waves induces limitations on the achievable performance. Further, the controller is applied to intended string movements, where control can be used to remove conservative limitations on the speed of the movement.

Keywords: Distributed-parameter systems, Disturbance rejection, Boundary control, Managed pressure drilling, Well control

1. INTRODUCTION

Maintaining the pressure in a borehole above the pore pressure and below the fracture pressure of the formation is essential for the safety of drilling operations. Therefore, a fluid called drilling mud is pumped down through the drill string, through the bit and up the annulus. The mud is designed such that the pressure remains within tolerable margins. For wells where the pressure margins are tight, so-called managed pressure drilling was developed, enabling fast active control of the annular pressure using a choke and backpressure pump at the outlet of the annulus, without having to change the mud properties (Godhavn et al. (2010)). However, drill string movements disturb the system and must be compensated for. Drill string movements occur due to the wave-induced heaving motion of a floating drilling rig, and during tripping. Tripping is the intentional movement of the string into or out of the well, e.g. in order to change the drilling equipment. We consider the attenuation of such string-movement induced pressure fluctuations using the choke and measurements that are available on the rig. This is one of several applications within drilling where the distributed dynamics of the system must be taken into account (Di Meglio and Aarsnes (2015)).

While drilling from a floating rig, a mechanical system decouples the rig's movement from the string. However, every 30 m the drill string must be fixed to the rig in order to extend it by another segment, and the string moves with the rig. The distributed dynamics of the heave problem were first addressed in Landet et al. (2013), and a controller was designed based on a discretized model. The heave disturbance is modeled as an inflow at the bottom. Most relevant to this work, a backstepping controller based on the 2×2 hyperbolic PDEs was developed in Aamo (2013), and this method was generalized in Anfinsen and Aamo (2015) to control the pressure at an arbitrary position in the well. However, their model neglects that the disturbance affects the system throughout the domain because fluid sticks to the drill string. Further, they consider only simplistic harmonic oscillations, and neglect that the heave can actually be measured on the rig using accelerometers. Thus, the disturbance does not need to be estimated from pressure and flow measurements, which improves the performance of the observer significantly.

String movements when tripping the drill string, or placing casing in the borehole, are actually more common, as they occur also when drilling from fixed platforms. A common procedure is to calculate the maximum velocity that results in tolerable pressure fluctuation (Mitchell (1988)). Active pressure control could increase the allowable speed, saving time.

The paper is organized as follows. In Section 2, we introduce the model, and in Section 3 we present the controller design. Three relevant simulation scenarios are discussed in Section 4. Finally, concluding remarks are given in Section 5.

2. MODELING

We consider the following model for the annular pressure and flow:

$$p_t(z,t) = -\frac{\beta}{A} q_z(z,t) \tag{1}$$

$$q_t(z,t) = -\frac{A}{\rho} p_z(z,t) - \frac{F}{\rho} q(z,t) + \frac{F_d}{\rho} v_d(z,t) - Ag \tag{2}$$

$$q(0,t) = -A_d v_d(0,t) \tag{3}$$

where $z \in [0,l]$, $t \geq 0$, l is the length of the well, $p(z,t)$ is pressure, $q(z,t)$ the volumetric flow rate, $v_d(z,t)$ is the drill string velocity, A the cross sectional area of the annulus, A_d is the area replaced by the drill string, β bulk modulus, ρ density, g the gravitational constant, F

⋆ Financial support from Statoil ASA is gratefully acknowledged.

and F_d are friction factors, and subscripts $_z$ and $_t$ denote derivatives with respect to space and time, respectively. The parameters A, β, ρ, F, and F_d can vary with z, but we omit this dependency for the sake of readability. The control objective is to control the bottomhole pressure to a given setpoint p_{sp}, i.e.

$$p(0,t) = p_{sp}. \tag{4}$$

The topside boundary condition is left as a control input. Model (1)-(2) for the annular dynamics was used in Aarsnes et al. (2013) for studying resonances and is an extension of the model that was used in Aamo (2013). The last term on the right-hand side of momentum balance (2) is added to model the "mud-clinging" effect: like in Couette flow, fluid sticks to the drill string, and via the viscous forces in the fluid the moving string induces a momentum on the fluid. We assume linear friction, which was shown to be reasonable for laminar flow of Newtonian fluids, and a limited frequency range in case of oscillations (Stecki and Davis (1986a), Stecki and Davis (1986b)). Thus, the drill string movement/disturbance enters the system not only as the inflow at the bottom of the hole, i.e. through a boundary condition, but also throughout the domain. The significance of the mud-clinging effect is illustrated in Section 4.1.

Simulations of the model in Aarsnes et al. (2013), which also contains drill string elasticity, have shown that the drill string is approximately rigid in most situations, unless the string's resonance frequency is excited for an extended period. Therefore, we assume that the velocity of the drill string equals the velocity at the rig, $v_d(z,t) = v_d(l,t)$ $\forall z \in [0,l]$, in which case the drill string velocity can be obtained from measurements on the rig. Thus, the estimation problem is significantly simplified compared to Aamo (2013).

2.1 Disturbance model

Due to the length of the well and the hyperbolic nature of the model, there is a delay between topside actuation and downhole effect. Therefore, the control involves feedforward using a prediction of the disturbance. This will be made precise in Section 3.2.

We consider two distinct cases of string movement. First, the string movement is intentional. In this case, the velocity is determined by the operator, i.e. it is known a priori. Second, we consider heave-induced oscillations. Here, the string velocity depends on the waves and the drilling rig's response. For this case, we consider the linear model

$$\dot{X}(t) = \bar{A}X(t), \tag{5}$$

$$v_{rig}(t) = \bar{C}X(t), \tag{6}$$

with

$$\bar{A} = diag\left(\begin{bmatrix} 0 & \omega_1 \\ -\omega_1 & 0 \end{bmatrix}, \dots \begin{bmatrix} 0 & \omega_n \\ -\omega_n & 0 \end{bmatrix}\right), \tag{7}$$

$$\bar{C} = [0\ 1\ \dots\ 0\ 1] \tag{8}$$

and $v_d(l,t) = v_{rig}(t)$. $X(t)$ can be estimated from measurements of v_{rig} using the observer

$$\dot{\hat{X}}(t) = \bar{A}\hat{X}(t) + L\left(v_{rig}(t) - \hat{v}_{rig}(t)\right), \tag{9}$$

$$\hat{v}_{rig}(t) = \bar{C}\hat{X}(t), \tag{10}$$

where the observer gain L is chosen such that $\bar{A} - L\bar{C}$ is Hurwitz. Heave prediction by this model is imperfect because sea waves are stochastic, and the n chosen frequencies $\omega_1, \dots, \omega_n$ do not cover the wave spectrum completely. However, we will assume that it suffices for obtaining short term predictions.

2.2 State transformation

In order to use previous results on backstepping controller design, it is desirable to bring system (1)-(3) on diagonal form. In Aamo (2013), Lemma 10, the coordinate transformation

$$u(x,t) = \frac{1}{2}\left(q(xl,t) + \frac{A}{\sqrt{\beta\rho}}(p(xl,t) - p_{sp} + \rho g l x)\right) \times e^{\frac{lF}{2\sqrt{\beta\rho}}x}, \tag{11}$$

$$v(x,t) = \frac{1}{2}\left(q(xl,t) - \frac{A}{\sqrt{\beta\rho}}(p(xl,t) - p_{sp} + \rho g l x)\right) \times e^{-\frac{lF}{2\sqrt{\beta\rho}}x}, \tag{12}$$

where $x \in [0,1]$, was given. In the presence of the additional term in (2) we get

$$u_t(x,t) = -\epsilon_1(x)u_x(x,t) + c_1(x)v(x,t) + d_1(x,t) \tag{13}$$

$$v_t(x,t) = \epsilon_2(x)v_x(x,t) + c_2(x)u(x,t) + d_2(x,t) \tag{14}$$

$$u(0,t) = qv(0,t) + d(t) \tag{15}$$

$$v(1,t) = U(t) \tag{16}$$

with

$$\epsilon_1 = \epsilon_2 = \frac{1}{l}\sqrt{\frac{\beta}{\rho}}, \qquad d(t) = -A_d v_d(0,t), \tag{17}$$

$$c_1(x) = -\frac{F}{2\rho}e^{\frac{lF}{\sqrt{\beta\rho}}x}, \qquad c_2(x) = -\frac{F}{2\rho}e^{-\frac{lF}{\sqrt{\beta\rho}}x}, \tag{18}$$

$$d_1(x,t) = \frac{F_d}{2\rho}e^{\gamma x}v_d(l,t), \quad d_2(x,t) = \frac{F_d}{2\rho}e^{-\gamma x}v_d(l,t), \tag{19}$$

$\gamma = \frac{lF}{2\sqrt{\beta\rho}}$ and $q = -1$. U is the control input to be designed. The control objective becomes

$$u(0,t) = rv(0,t) \tag{20}$$

with $r = 1$. For (1)-(2), the control law is realized by

$$q_l(t) = \frac{A}{\sqrt{\beta\rho}}(p_l(t) - p_{sp} + \rho g l) + 2U(t)e^{\frac{lF}{2\sqrt{\beta\rho}}}. \tag{21}$$

The first term is in the form of a "passive" boundary condition and is responsible for avoiding reflections of pressure waves, while the latter term involving U is the active control input.

The model for v_d remains unchanged. In case of a linear model of the form (5)-(6), the disturbance model is

$$\dot{X}(t) = AX(t), \tag{22}$$

$$d(t) = CX(t), \tag{23}$$

$$d_1(x,t) = C_1(x)X(t), \tag{24}$$

$$d_2(x,t) = C_2(x)X(t), \tag{25}$$

where $A = \bar{A}$, $C = -A_d\bar{C}$, $C_1(x) = \frac{F_d}{2\rho}e^{\frac{lF}{2\sqrt{\beta\rho}}x}\bar{C}$, and $C_2(x) = \frac{F_d}{2\rho}e^{-\frac{lF}{2\sqrt{\beta\rho}}x}\bar{C}$ in our case, and X can be estimated using (9) - (10). More generally, the method in this paper can also be applied for any nonlinear disturbance model that provides a prediction of the disturbance. The requirements on the prediction are made precise in Section 3.2.

3. CONTROLLER DESIGN

3.1 Backstepping transformation

The backstepping transformation

$$\begin{aligned}\alpha(x,t) =& u(x,t) - \int_0^x K^{uu}(x,\xi)u(\xi,t)d\xi \\ &- \int_0^x K^{uv}(x,\xi)v(\xi,t)d\xi,\end{aligned} \tag{26}$$

$$\begin{aligned}\beta(x,t) =& v(x,t) - \int_0^x K^{vv}(x,\xi)v(\xi,t)d\xi \\ &- \int_0^x K^{vu}(x,\xi)u(\xi,t)d\xi\end{aligned} \tag{27}$$

was introduced in Vazquez et al. (2011) to map the system without disturbances into a target system, where the kernels satisfy the partial differential equations

$$\begin{aligned}&\epsilon_1(x)K^{uu}_x(x,\xi) + \epsilon_1(\xi)K^{uu}_\xi(x,\xi) \\ &\quad = -\epsilon_1'(\xi)K^{uu}(x,\xi) - c_2(\xi)K^{uv}(x,\xi)\end{aligned} \tag{28}$$

$$\begin{aligned}&\epsilon_1(x)K^{uv}_x(x,\xi) - \epsilon_2(\xi)K^{uv}_\xi(x,\xi) \\ &\quad = \epsilon_2'(\xi)K^{uv}(x,\xi) - c_1(\xi)K^{uu}(x,\xi)\end{aligned} \tag{29}$$

$$\begin{aligned}&\epsilon_2(x)K^{vu}_x(x,\xi) - \epsilon_1(\xi)K^{vu}_\xi(x,\xi) \\ &\quad = \epsilon_1'(\xi)K^{vu}(x,\xi) + c_2(\xi)K^{vv}(x,\xi)\end{aligned} \tag{30}$$

$$\begin{aligned}&\epsilon_2(x)K^{vv}_x(x,\xi) + \epsilon_2(\xi)K^{vv}_\xi(x,\xi) \\ &\quad = -\epsilon_2'(\xi)K^{vv}(x,\xi) + c_1(\xi)K^{vu}(x,\xi)\end{aligned} \tag{31}$$

on $\mathcal{T} = \{(x,\xi) : 0 \le \xi \le x \le 1\}$ and boundary conditions

$$K^{uu}(x,0) = \frac{\epsilon_2(0)}{q\epsilon_1(0)}K^{uv}(x,0) \tag{32}$$

$$K^{uv}(x,x) = \frac{c_1(x)}{\epsilon_1(x)+\epsilon_2(x)} \tag{33}$$

$$K^{vu}(x,x) = -\frac{c_2(x)}{\epsilon_1(x)+\epsilon_2(x)} \tag{34}$$

$$K^{vv}(x,0) = \frac{q\epsilon_1(0)}{\epsilon_2(0)}K^{vu}(x,0). \tag{35}$$

In the presence of the disturbances, and using the control input

$$U(t) = V(t) + \int_0^1 K^{vu}(1,\xi)u(\xi,t) + K^{vv}(1,\xi)v(\xi,t)d\xi, \tag{36}$$

transformation (26)-(27) maps the system (13)-(16) into

$$\begin{aligned}\alpha_t(x,t) =& -\epsilon_1(x)\alpha_x(x,t) - \epsilon_1(0)K^{uu}(x,0)d(t) \\ &+ d_1(x,t) - \int_0^x K^{uu}(x,\xi)d_1(\xi,t)d\xi \\ &- \int_0^x K^{uv}(x,\xi)d_2(\xi,t)d\xi,\end{aligned} \tag{37}$$

$$\begin{aligned}\beta_t(x,t) =& \epsilon_2(x)\beta_x(x,t) - \epsilon_1(0)K^{vu}(x,0)d(t) \\ &+ d_2(x,t) - \int_0^x K^{vu}(x,\xi)d_1(\xi,t)d\xi \\ &- \int_0^x K^{vv}(x,\xi)d_2(\xi,t)d\xi,\end{aligned} \tag{38}$$

$$\alpha(0,t) = q\beta(0,t) + d(t), \tag{39}$$

$$\beta(1,t) = V(t), \tag{40}$$

which can be shown by following the steps in the proof of Lemma 1 in Aamo (2013). Since $\alpha(0,t) = u(0,t)$ and $\beta(0,t) = v(0,t)$, the control objective becomes

$$\alpha(0,t) = r\beta(0,t). \tag{41}$$

Using Lemma 2 in Aamo (2013), the explicit solution to (37) and (38) can be obtained. With

$$h_\alpha(z) = \int_z^1 \frac{1}{\epsilon_1(\gamma)}d\gamma, \qquad d_\alpha = h_\alpha(0), \tag{42}$$

$$h_\beta(z) = \int_z^1 \frac{1}{\epsilon_2(1-\gamma)}d\gamma, \qquad d_\beta = h_\beta(0), \tag{43}$$

$$\begin{aligned}f_\beta(x,t) =& -\epsilon_1(0)K^{vu}(x,0)d(t) + d_2(x,t) \\ &- \int_0^x K^{vu}(x,\xi)d_1(\xi,t)d\xi - \int_0^x K^{vv}(x,\xi)d_2(\xi,t)d\xi,\end{aligned} \tag{44}$$

the solution to (38) satisfies

$$\beta(0,t) - \beta(1,t-d_\alpha) = \int_{t-d_\alpha}^t f_\beta(1-h_\beta^{-1}(t-\gamma),\gamma)d\gamma. \tag{45}$$

For the linear disturbance model (22)-(25), f_β becomes linear in the disturbance state $X(t)$, and there is a separation between space and time-varying terms:

$$\begin{aligned}f_\beta(x,t) =& \Big[-\epsilon_1(0)K^{vu}(x,0)C + C_2(x) \\ &- \int_0^x K^{vu}(x,\xi)C_1(\xi) + K^{vv}(x,\xi)C_2(\xi)d\xi \Big] X(t) \\ =:& K_\beta(x)X(t).\end{aligned} \tag{46}$$

Using this, the analogue to (45) is

$$\beta(0,t) - \beta(1,t-d_\beta) = \int_0^{d_\beta} K_\beta(1-h_\beta^{-1}(\tau),0)e^{-A\tau}d\tau X(t). \tag{47}$$

Similar calculations can be done for the α-system, but they are not required here.

3.2 Controller design

Using (39), (40), and (45), we get

$$\begin{aligned}\alpha(0,t) =& q\beta(0,t) + d(t) \\ =& r\beta(0,t) + (q-r)\beta(0,t) + d(t) \\ =& r\beta(0,t) + (q-r)V(t-d_\beta) + d(t) \\ &+ (q-r)\int_{t-d_\beta}^t f_\beta(1-h_\beta^{-1}(t-\gamma),\gamma)d\gamma.\end{aligned} \tag{48}$$

The control objective (41) is achieved if and only if (setting the sum of all but the first term on the right-hand side zero and shifting time)

$$\begin{aligned}V(t) =& -\frac{1}{q-r}d(t+d_\beta) \\ &+ \int_t^{t+d_\beta} f_\beta(1-h_\beta^{-1}(t+d_\beta-\gamma),\gamma)d\gamma.\end{aligned} \tag{49}$$

Thus, the control input at time t requires knowledge of the disturbances at all times $\tau \in [t, t+d_\beta]$, i.e. d_β into the future. This can be implemented using a disturbance prediction as discussed in Section 2. For the linear disturbance

model, V can be implemented as (using the predicted disturbance $\tilde{X}(t+\tau) = e^{A\tau}\hat{X}(t)$)

$$V(t) = -\frac{1}{q-r}Ce^{Ad_\beta}\hat{X}(t) - \int_0^{d_\beta} K_\beta(1-h_\beta^{-1}(\tau))e^{A(d_\beta-\tau)}d\tau\hat{X}(t). \tag{50}$$

As mentioned earlier, there can be a mismatch between predicted and actual disturbances, resulting in an error in the control objective. For the linear case, inserting (50) into (48) yields

$$\begin{aligned} u(0,t) =& rv(0,t) + \left(d(t) - Ce^{Ad_\beta}\hat{X}(t-d_\beta)\right) \\ &+ (q-r)\left(\int_{t-d_\beta}^{t} f_\beta(1-h_\beta^{-1}(t-\gamma),\gamma)d\gamma \right. \\ &\left. - \int_0^{d_\beta} K_\beta(1-h_\beta^{-1}(\tau))e^{A(d_\beta-\tau)}d\tau\hat{X}(t-d_\beta)\right). \end{aligned} \tag{51}$$

This illustrates how a prediction error in the disturbance imposes limitations on the achievable controller performance.

3.3 Observer

To implement (36), u and v are required throughout the domain. In practice, only measurements at the right boundary are available. Therefore, we use the observer

$$\begin{aligned} \hat{u}_t(x,t) &= -\epsilon_1(x)\hat{u}_x(x,t) + c_1(x)\hat{v}(x,t) + d_1(x,t) \\ &\quad + p_1(x)(u(1,t) - \hat{u}(1,t)) && (52) \\ \hat{v}_t(x,t) &= \epsilon_2(x)\hat{v}_x(x,t) + c_2(x)\hat{u}(x,t) + d_2(x,t) \\ &\quad + p_2(x)(u(1,t) - \hat{u}(1,t)) && (53) \\ \hat{u}(0,t) &= q\hat{v}(0,t) + d(t) && (54) \\ \hat{v}(1,t) &= U(t), && (55) \end{aligned}$$

where p_1 and p_2 are output injection gains to be designed. Forming error equations by subtracting (52)-(55) from (13)-(16) yields the error system

$$\begin{aligned} \tilde{u}_t(x,t) &= -\epsilon_1(x)\tilde{u}_x(x,t) + c_1(x)\tilde{v}(x,t) - p_1(x)\tilde{u}(1,t) && (56) \\ \tilde{v}_t(x,t) &= \epsilon_2(x)\tilde{v}_x(x,t) + c_2(x)\tilde{u}(x,t) - p_2(x)\tilde{u}(1,t) && (57) \\ \tilde{u}(0,t) &= q\tilde{v}(0,t) && (58) \\ \tilde{v}(1,t) &= 0. && (59) \end{aligned}$$

Note that the disturbance terms cancel. Therefore, the observer in Vazquez et al. (2011) can be applied. The observer error becomes zero within $d_\alpha + d_\beta$. The output injection gains p_1 and p_2 are obtained by solving observer kernel PDEs similar to (28)-(35). They are given in Vazquez et al. (2011).

4. SIMULATIONS

In this section, we present examples to illustrate the performance of the controller. The following common parameters are used

$$\begin{aligned} \beta &= 1.6\times10^9\,\text{Pa}, & \rho &= 1420\,\text{kg/m}^3, \\ A_d &= 0.0127\,\text{m}^2, & \mu &= 42\,\text{mPas}, \\ A &= 0.0198\,\text{m}^2, & F &= 700\,\text{kg/m}^3\text{s}, \end{aligned}$$

The friction factor F was calculated using a modification of the Hagen-Poisseuille law for the annular geometry and viscosity μ , and $F_d = 0.5AF$. The length l varies in the examples. The pressure setpoint was set to a value slightly above the hydrostatic pressure, $p_{sp} = 1.05\rho gl$, but this does not affect the dynamics.

4.1 Mud-clinging effect

In this example, we compare the controller (50) with the controller from Aamo (2013) in the presence of the mud-clinging effect. In order to isolate the effect of the additional momentum term, we assume a sinusoidal (i.e. predictable) heave motion with period 12 s and amplitude 1 m, $v_{rig} = 2\pi a\sin(\omega t)$ ($\omega = \frac{2\pi}{12}$ and $a = 1$), and use $l = 2000$ m.

In Figure 1, the downhole pressure regulation error $p(0,t)$ is depicted for three cases: controller (50), the controller from Aamo (2013), and $U(t) \equiv 0$ for comparison. The controller neglecting the mud-clinging effect achieves a clear reduction compared to no control, but significant pressure fluctuations remain.

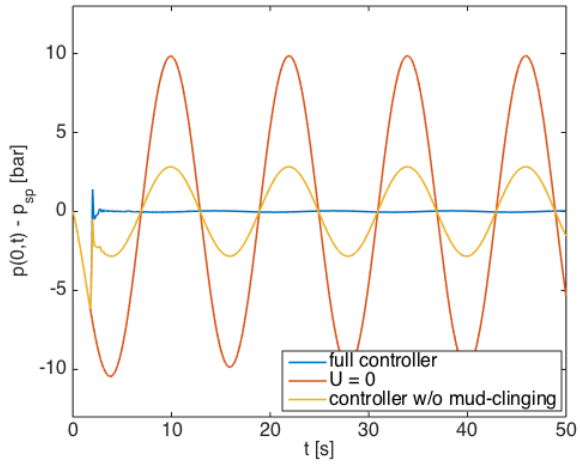

Fig. 1. Downhole pressure oscillations using controller (50), the controller from Aamo (2013), and using no control ($U = 0$).

4.2 Real heave data

Heave measurements from a semisubmersible rig are depicted in Figure 2. This is a typical heave spectrum for a rig operated in the North Sea, where high-frequency components are dampened by the rig. The heave velocity is estimated using (9) - (10), where the frequencies $\omega_1, \ldots, \omega_5$ are chosen according to the velocity's frequency spectrum, see Figure 3. In practice, the spectrum can be updated regularly to match the current sea state. A time series of the resulting pressure oscillations in a 5000 m long well is depicted in Figure 4. The controller succeeds in reducing the pressure fluctuations at the bottom of the well, but some oscillations remain due to the error in the disturbance prediction. Motivated by (51), measured and predicted rig velocities are compared in Figure (2), where the predicted velocity is given by

$$\tilde{v}_{rig}(t) = \bar{C}e^{\bar{A}T}\hat{X}(t-T) \tag{60}$$

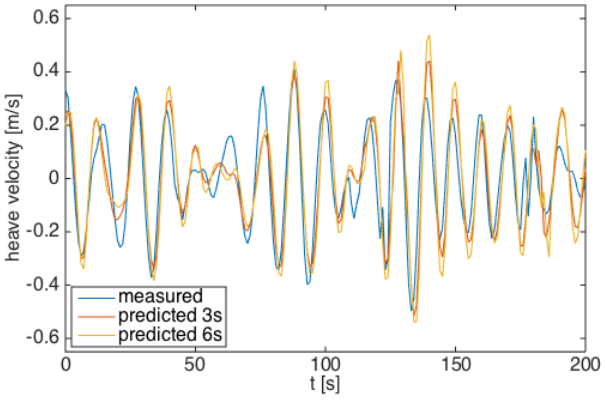

Fig. 2. Measured heave velocity and predicted velocity using (60) for $T = 3,6\,\mathrm{s}$.

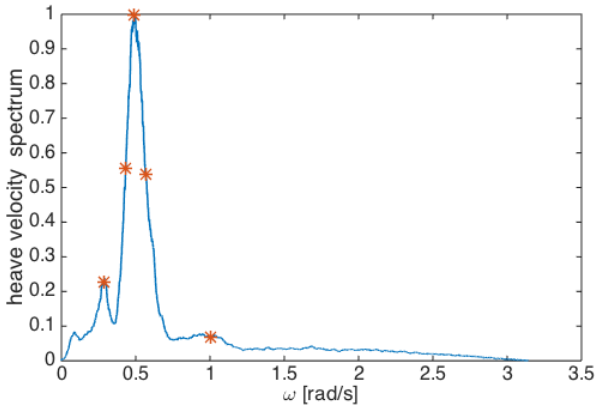

Fig. 3. Heave velocity spectrum and chosen frequencies.

for the prediction horizon T. The cummulative distribution functions of the downhole pressure oscillations for different well lengths are depicted in Figure 5. Clearly, the pressure variations increase with well length, because of the longer prediction. Note that these values can be computed directly from Equation (51). The distribution function without active control ($U = 0$), which is almost independent from l, is depicted for comparison. Considering that uncertainties and practical challenges in the implementation of controller (50) increase the pressure variations, one needs to assess the advantages compared to the simpler strategy $U = 0$ for long wells. The root mean square as another measure of the downhole pressure variation is depicted in Figure 6. More relevant in practice is the maximum deviation from p_{sp}. The figure shows that the maximum varies little with l and attains already a high value at short lengths. However, maxima over a short time might have little effect due to the plasticity of the formation. Therefore,

$$\frac{1}{T}\int_0^T (|p(0,t) - p_{sp}| - 2.5) \times \mathbb{1}_{|p(0,t)-p_{sp}|>2.5} dt \qquad (61)$$

can be used as a measure for the "energy" per time beyond the margin $p_{sp} \pm 2.5$ bar that is applied to the formation. The figure shows that this energy increases significantly for $l > 6000$ although the maximum remains approximately constant. Figures 5 and 6 can be used to judge if the pressure oscillations are tolerable based on the expected, or currently observed, heave motion.

4.3 Intended drill string movements

Another interesting scenario is when running the drill string, or casing, into or pulling it out of the borehole. A common procedure is to estimate the maximum velocity that results in a tolerable surge or swab pressure, respectively, see e.g. Mitchell (1988). Control could be used to actively attenuate these pressure fluctuations, allowing a higher tripping speed. This case serves as an example where the string velocity is known a priori. The controller in this paper is designed on the assumption that string movement causes a flow at the bottom. This assumption is satisfied at least for the lowermost string segments.

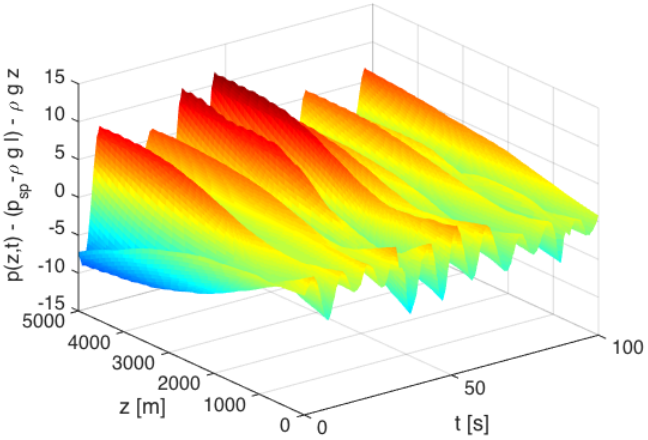

Fig. 4. Pressure deviation from steady conditions for real heave data and $l = 5000\,\mathrm{m}$.

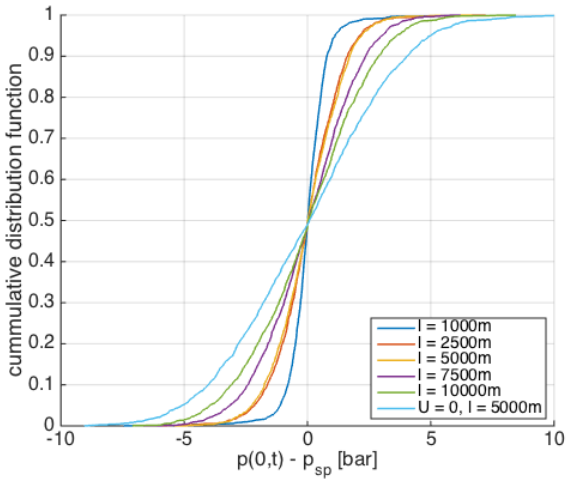

Fig. 5. Cummulative distribution function of the downhole pressure regulation error for different well lengths and $U = 0$ for comparison.

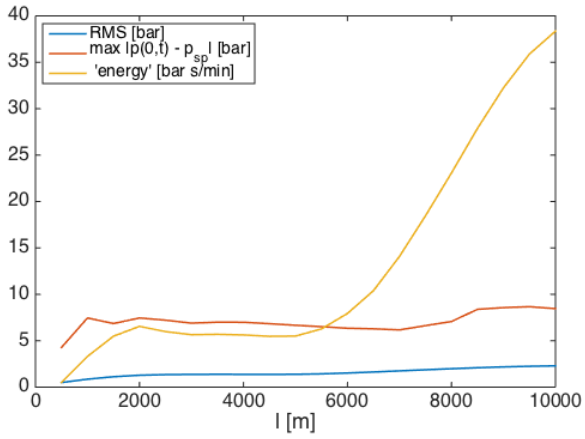

Fig. 6. Root mean square, maximum value and "energy" as defined in (61) of the downhole pressure regulation error over well length.

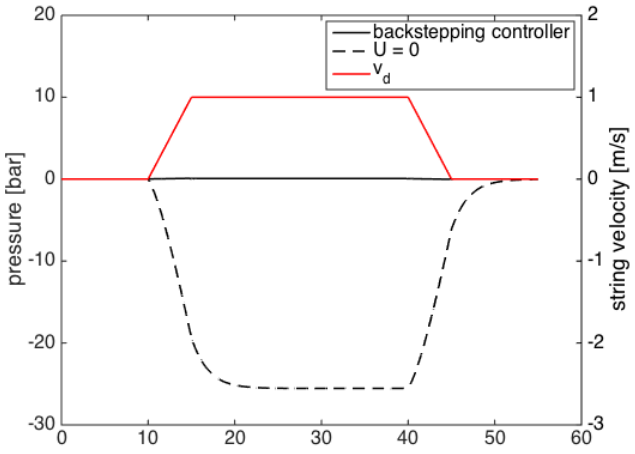

Fig. 7. Bottomhole pressure when pulling the drill string with and without control.

For a given string velocity, pressure fluctuations increase with decreasing clearance between drill string and borehole wall. The clearance is smallest in deep parts of a well, because the well diameter decreases with each casing that is installed. Also, the bottom is the most pressure sensitive part of a well, because the upper parts have been protected by casing and cement. Therefore, the most relevant case is when the bit is relatively close to the bottom, see also Mitchell (2004). Judging how far the string may be off bottom is beyond the scope of this paper. Figure 7 shows the bottomhole pressure where the drill string is pulled by one segment (30m) with a maximum velocity of 1 m/s. The pressure deviation without control would be too severe in certain cases, while the backstepping controller attenuates all pressure fluctuations.

5. CONCLUSIONS

We have extended previous results on backstepping control of 2×2 linear hyperbolic PDEs to attenuate disturbances appearing at the boundary and throughout the domain. The method was applied to pressure control in drilling. The control law requires a prediction of the disturbance that can be obtained either from a schedule of an intentional string movement or from a model. Limits on controller performance due to unpredictability of the disturbance have been investigated. Further work could include improving the prediction of the velocity in the heave problem, e.g. by heave measurements in some distance around the rig. The drill string dynamics could be included in the model and controller design to relax the assumption of rigidity. For this purpose, results in Hu et al. (2015) might be exploited. To allow control when the string is far off bottom, the controller could be modified to allow inflow within the domain. Finally, uncertainty in bulk modulus and friction parameters should be explored.

REFERENCES

Aamo, O.M. (2013). Disturbance rejection in 2 x 2 linear hyperbolic systems. *IEEE Transactions on Automatic Control*, 58(5), 1095–1106.

Aarsnes, U.J.F., Aamo, O.M., Hauge, E., and Pavlov, A. (2013). Limits of controller performance in the heave disturbance attenuation problem. In *2013 European Control Conference (ECC)*, 1071–1076.

Anfinsen, H. and Aamo, O.M. (2015). Disturbance rejection in the interior domain of linear 2 2 hyperbolic systems. *IEEE Transactions on Automatic Control*, 60(1), 186–191.

Di Meglio, F. and Aarsnes, U. (2015). A distributed parameter systems view of control problems in drilling. In *2nd IFAC Workshop on Automatic Control in Offshore Oil and Gas Production, Florianópolis, Brazil*.

Godhavn, J.M. et al. (2010). Control requirements for automatic managed pressure drilling system. *SPE Drilling & Completion*, 25(03), 336–345.

Hu, L., Di Meglio, F., Vazquez, R., and Krstic, M. (2015). Control of homodirectional and general heterodirectional linear coupled hyperbolic pdes. *arXiv preprint arXiv:1504.07491*.

Landet, I.S., Pavlov, A., and Aamo, O.M. (2013). Modeling and control of heave-induced pressure fluctuations in managed pressure drilling. *IEEE Transactions on Control Systems Technology*, 21(4), 1340–1351.

Mitchell, R. (1988). Dynamic surge/swab pressure predictions. *SPE drilling engineering*, 3(03), 325–333.

Mitchell, R.F. (2004). Surge pressures in low-clearance liners. In *2004 IADC/SPE Drilling Conference*. Society of Petroleum Engineers.

Stecki, J. and Davis, D. (1986a). Fluid transmission lines-distributed parameter models part 1: A review of the state of the art. *Proceedings of the Institution of Mechanical Engineers, Part A: Journal of Power and Energy*, 200(4), 215–228.

Stecki, J. and Davis, D. (1986b). Fluid transmission lines-distributed parameter models part 2: comparison of models. *Proceedings of the Institution of Mechanical Engineers, Part A: Journal of Power and Energy*, 200(4), 229–236.

Vazquez, R., Krstic, M., and Coron, J.M. (2011). Backstepping boundary stabilization and state estimation of a 2× 2 linear hyperbolic system. In *2011 50th IEEE Conference on Decision and Control and European Control Conference (CDC-ECC)*, 4937–4942.